JCTC Journal of Chemical Theory and Computation

ARTICLE

pubs.acs.org/JCTC

Generalized Gradient Approximations of the Noninteracting Kinetic Energy from the Semiclassical Atom Theory: Rationalization of the Accuracy of the Frozen Density Embedding Theory for Nonbonded Interactions

S. Laricchia,[†] E. Fabiano,[‡] L. A. Constantin,[†] and F. Della Sala*[,†,‡]

[†]Center for Biomolecular Nanotechnologies @UNILE, Istituto Italiano di Tecnologia (IIT), Via Barsanti, 73010 Arnesano (LE), Italy

[‡]National Nanotechnology Laboratory (NNL), Istituto Nanoscienze-CNR, Via per Arnesano 16, 73100 Lecce, Italy

Supporting Information

ABSTRACT: We present a new class of noninteracting kinetic energy (KE) functionals, derived from the semiclassical-atom theory. These functionals are constructed using the link between exchange and kinetic energies and employ a generalized gradient approximation (GGA) for the enhancement factor, namely, the Perdew−Burke−Ernzerhof (PBE) one. Two of them, named APBEK and revAPBEK, recover in the slowly varying density limit the modified second-order gradient (MGE2) expansion of the KE, which is valid for a neutral atom with a large number of electrons. APBEK contains no empirical parameters, while revAPBEK has one empirical parameter derived from exchange energies, which leads to a higher degree of nonlocality. The other two functionals, APBEKint and revAPBEKint, modify the APBEK and revAPBEK enhancement factors, respectively, to recover the second-order gradient expansion (GE2) of the homogeneous electron gas. We first benchmarked the total KE of atoms/ions and jellium spheres/surfaces: we found that functionals based on the MGE2 are as accurate as the current state-of-the-art KE functionals, containing several empirical parameters. Then, we verified the accuracy of these new functionals in the context of the frozen density embedding (FDE) theory. We benchmarked 20 systems with nonbonded interactions, and we considered embedding errors in the energy and density. We found that all of the PBE-like functionals give accurate and similar embedded densities, but the revAPBEK and revAPBEKint functionals have a significant superior accuracy for the embedded energy, outperforming the current state-of-the-art GGA approaches. While the revAPBEK functional is more accurate than revAPBEKint, APBEKint is better than APBEK. To rationalize this performance, we introduce the reduced-gradient decomposition of the nonadditive kinetic energy, and we discuss how systems with different interactions can be described with the same functional form.

1. INTRODUCTION

Density functional theory (DFT)[1−3] is one of the most widely used approaches for theoretical calculations in solid-state physics[4] and quantum-chemistry.[5] In its original orbital-free (OF) formulation,[6,7] DFT allows one to describe the ground state of a many-electron system as a function of the electron density (ρ) alone, through the solution of the Euler equation:[2]

$$\frac{\delta T_s[\rho]}{\delta\rho(\mathbf{r})} + v_{ext}(\mathbf{r}) + v_J(\mathbf{r};[\rho]) + \frac{\delta E_{xc}[\rho]}{\delta\rho(\mathbf{r})} = \mu \qquad (1)$$

where $T_s[\rho]$ is the noninteracting kinetic energy (KE) density functional; $v_{ext}(\mathbf{r})$ and $v_J(\mathbf{r};[\rho])$ are the external (i.e., nuclear) and Coulomb potentials, respectively; $E_{xc}[\rho]$ is the exchange-correlation (XC) energy functional; and the Lagrange multiplier μ is the chemical potential, which takes into account that the number of electrons is fixed.

Equation 1 is of limited practical utility, since only $v_J(\mathbf{r};[\rho])$ is known as an explicit functional of the electron density, while the exact functional forms of $T_s[\rho]$ and $E_{xc}[\rho]$ are not known. For the XC term, many different successful approximations have been developed for different kinds of systems (molecules,[8] solids,[9,10] surfaces,[10] interfaces,[11,12] etc.), mainly taking advantage of the fact that E_{xc} is by far the smallest term in eq 1. For the noninteracting kinetic energy functional, on the contrary, reliable approximations are still lacking. For this reason, OF-DFT calculations have been so far only performed for selected solid-state systems,[7,13−20] and DFT calculations are instead routinely performed within the Kohn−Sham (KS) scheme.[1] This requires, however, the introduction of orthonormalized orbitals and implies a formal $\mathcal{O}(N^3)$ scaling.

In recent years, further interest in the KE functionals and related approximations has been motivated by the development of density-based embedding methods[21−33] and, in particular, the frozen density embedding (FDE).[25] In the FDE approach, a many-electron system with electron density ρ is partitioned into two subsystems A and B, such that the total electron density is $\rho = \rho_A + \rho_B$. The KS equations of subsystem A under the influence of subsystem B (or equivalently those of subsystem B under the influence of A) can be solved exactly within the FDE formalism if the embedding (local) potential

$$v_{emb}(\mathbf{r},[\rho_A;\rho_B]) = v_{ext}^B(\mathbf{r}) + v_J(\mathbf{r};[\rho_B]) + \frac{\delta E_{xc}^{nadd}[\rho_A;\rho_B]}{\delta\rho_A(\mathbf{r})} + \frac{\delta T_s^{nadd}[\rho_A;\rho_B]}{\delta\rho_A(\mathbf{r})} \qquad (2)$$

is added to the standard KS equations. In eq 2, $v_{ext}^B(\mathbf{r})$ and $v_J(\mathbf{r};[\rho_B])$ are respectively the external (i.e., nuclear) and the Coulomb potentials due to subsystem B, and the nonadditive XC and kinetic energy

Received: June 7, 2011
Published: July 08, 2011

terms are

$$\begin{aligned} E_{xc}^{nadd}[\rho_A,\rho_B] &= E_{xc}[\rho_A + \rho_B] - E_{xc}[\rho_A] - E_{xc}[\rho_B] \\ T_s^{nadd}[\rho_A,\rho_B] &= T_s[\rho_A + \rho_B] - T_s[\rho_A] - T_s[\rho_B] \end{aligned} \quad (3)$$

For the nonadditive XC energy (and potential), generalized gradient approximations (GGA) are often successfully employed. For the nonadditive kinetic energy (and potential), accurate approximations expressing T_s as a functional of the electron density are needed. Actually, for molecular systems, GGA approximations of T_s only provide good accuracy for FDE calculations for subsystems with nonbonded interactions,[34−38] while strongly interacting systems or charge-transfer interactions cannot be properly described.[37−39] Despite these shortcomings, GGA functionals are the method of choice for, e.g., biological systems: in this context, weak interactions dominate, and FDE can outperform current hybrid quantum mechanics/molecular mechanics (QM/MM) empirical models.[40]

Exact KE functionals are well-known for the homogeneous electron gas, i.e., the Thomas−Fermi (TF) local functional,[41,42] and for one- and two-electron systems, i.e., the von Weizsäcker[43] functional. In between these two extreme cases, different semilocal[44−53] or nonlocal[14,17,18,54−58] approximations were derived in recent years. Nonlocal KE functionals are rather accurate, but they are derived mainly from the linear response of the homogeneous electron gas (the Lindhard function[3]) and are thus only suitable for solid-state simulations. Semilocal KE functionals are instead usually developed on the basis of the generalized gradient expansion or its resummation (for recent reviews, see refs 38 and 59).

The development of GGA KE functionals was also guided by the so-called *conjointness conjecture*, which expresses a hypothetical link between exchange and kinetic energy functionals.[60−62] Therefore, semilocal KE approximations were constructed with the general form

$$T_s[\rho] = \int \mathrm{d}\mathbf{r}\, \tau_s^{HEG}(\rho)\, F_s(s) \quad (4)$$

with $\tau_s^{HEG} = 3/10(3\pi^2)^{2/3}\rho^{5/3}$ being the kinetic energy density of the homogeneous electron gas (HEG),[41,42] $s = |\nabla\rho|/\{2(3\pi^2)^{1/3}\rho^{4/3}\}$ being the dimensionless gradient, and F_s being a suitable kinetic enhancement factor resembling a corresponding exchange enhancement factor. We note that, because of the spin scaling relations,[63] the exchange and kinetic energies for a spin-polarized system can be evaluated from the spin-unpolarized versions, so in this paper, we only use equations for spin-unpolarized systems. In addition, unless otherwise stated, atomic units are used throughout, i.e., $e^2 = \hbar = m_e = 1$.

Following the approach outlined above, Lembarki and Chermette[64] constructed a GGA kinetic energy functional (named LC94 or PW91K) using for the enhancement factor the same form as the Perdew−Wang (PW91)[65] exchange functional:

$$F_s^{LC94}(s) = \frac{1 + a_1 s \operatorname{arcsinh}(a_2 s) + (a_3 - a_4\, e^{a_5 s^2})s^2}{1 + a_1 s \operatorname{arcsinh}(a_2 s) + a_6 s^4} \quad (5)$$

where the parameters $a_1 = 0.093907$, $a_2 = 76.32$, $a_3 = 0.26608$, $a_4 = 0.0809615$, $a_5 = -100$, and $a_6 = 0.57767 \times 10^{-4}$ were refitted to kinetic energies of atoms. For a slowly varying density, LC94 formally recovers the correct second-order gradient expansion (GE2)[66] and is considered one of the most accurate GGA functionals for FDE simulations of weakly bounded molecular systems.[27,34,38,67] Later, Tran and Wesolowski[68] constructed a PBE-like functional (named TW02) for the kinetic energy, with an enhancement factor of the form

$$F_s^{PBE}(s) = 1 + \kappa_s - \frac{\kappa_s}{1 + \frac{\mu_s s^2}{\kappa_s}} \quad (6)$$

where $\kappa_s = 0.8438$ and $\mu_s = 0.2319$ were fitted to the kinetic energies of various noble gases. The TW02 functional also shows very good performance for FDE calculations of weakly interacting molecules.[38] For a complete list of KE functionals based on the conjointness conjecture, see refs 38, 59, and 69.

Recently,[70] we proposed two different PBE-like approximations for the KE (APBEK and revAPBEK) based on the conjointness conjecture and the semiclassical atom reference system.[71] In these approximations, the value of $\mu_s = 0.23899$ was not obtained empirically from a fit but fixed by imposing exact constraints on the KE. In APBEK, the value of $\kappa_s = 0.804$ was also fixed nonempirically, by numerical analysis of the KE of heavy atoms, and it coincides with the one used in the PBE exchange (fixed by the Lieb-Oxford bound[8,70]). In revAPBEK, the value of κ_s was obtained in analogy with the revised PBE exchange[72] ($\kappa_s = 1.245$), and it was found that this value leads to very accurate FDE energies for eight weakly interacting systems, outperforming LC94.[70]

In this paper, we develop further the work of ref 70 and discuss in detail the performance of the APBEK and revAPBEK functionals for a larger set of systems within the FDE theory. Moreover, we introduce new PBE-like KE approximations (named revAPBEKint and APBEKint) which recover the correct second-order gradient expansion coefficient μ_s^{GE2} in the slowly varying density regime. The APBEKint/revAPBEKint functionals are developed in the spirit of the conjointness conjecture following the approach used in the development of the PBEint exchange functional[11] (which solves the analogous problem for the exchange and provides a link between the rapidly and slowly varying density regimes). The APBEKint/revAPBEKint functionals show, in general, performances close to the ones of APBEK/revAPBEK. However, for various tests, differences are significant. A direct comparison of these four PBE-like functionals allows us to rationalize the importance of the enhancement factor for small and large reduced gradients. To this end, we introduce the reduced-gradient decomposition of the nonadditive kinetic energy (see section 3.3).

The paper is organized as follows: In section 2, we explain the APBEK and revAPBEK constructions, and we present the revAPBEKint and APBEKint KE functionals. Section 3 reports computational details and the definition of the reduced-gradient decomposition. In section 4.1, we test the performance of our functionals to compute the total kinetic energy of 51 atoms and ions, jellium spheres, and surfaces. In section 4.2, we apply them to compute the nonadditive kinetic energy and potential in FDE calculations of 20 molecular systems with different kinds of nonbonded interactions: dispersion, dipole−dipole, and hydrogen bonds. Finally, in section 6, conclusions are drawn.

2. THEORY

2.1. The Large-*Z* Asymptotic Expansion of the Kinetic Energy. For many-electron nonrelativistic neutral atoms, the noninteracting kinetic energy has the following asymptotic

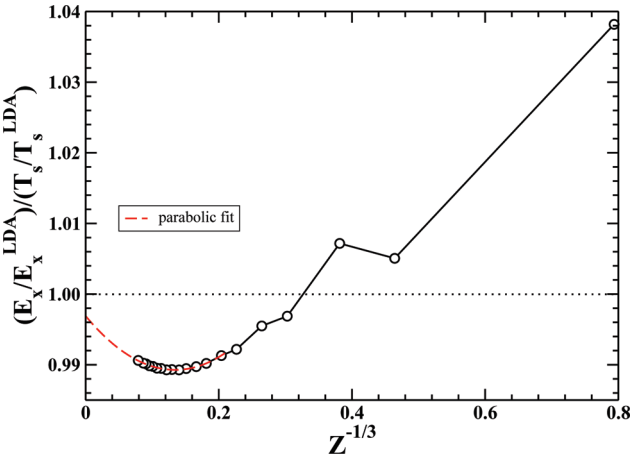

Figure 1. Comparison between exchange and kinetic energies for noble gases.

expansion

$$T_s = c_0 Z^{7/3} + c_1 Z^2 + c_2 Z^{5/3} + \ldots \quad (7)$$

where Z is the number of electrons, $c_0 = 0.768745$ is given by the Thomas−Fermi theory,[41,42] $c_1 = -0.5$ is the Scott correction,[73] and $c_2 = 0.2699$ was found in the semiclassical theory.[74,75] Equation 7 is very accurate, even for a small Z, with a typical error on the order of 0.2−0.5%[76] for atoms of the periodic table with $Z > 6$. The coefficients of the asymptotic expansion (eq 7) cannot be recovered from GE2 with $\mu_s^{GE2} = 5/27 = 0.185$[66] ($c_1^{GE2} = -0.5362$ and $c_2^{GE2} = 0.3360$ are obtained[76]), but the c_1 coefficient is exactly recovered by the modified second-order gradient expansion (MGE2)[76]

$$T_s^{MGE2}[\rho] = \int \mathrm{d}\mathbf{r}\, \tau_s^{HEG}[\rho](1 + \mu_s^{MGE2} s^2) \quad (8)$$

with $\mu_s^{MGE2} = 0.23899$.

For the c_2 coefficient, gradient expansions are less useful,[76] and $c_2 = 0.3217$ is found from MGE2, slightly better than GE2. Since MGE2 yields exactly the c_1 coefficient of eq 7 and for most systems the important energetic region is $s \leq 2$, we can expect any reasonable functional reducing to MGE2 in the small-s limit to reproduce fairly well eq 7 and thus to be rather accurate for the KE of atoms.

2.2. The Conjointness Conjecture. In ref 70, we discussed the relation between the kinetic and exchange enhancement factors. In order to understand this link better, we report in Figure 1 the ratio $(E_x^{exact}/E_x^{LDA})/(T_s^{exact}/T_s^{LDA})$ for nonrelativistic noble gas atoms with $Z = 2$ to $Z = 2022$. (Here, LDA is the popular acronym for the local density approximation.[1]) We also extrapolate the curve to $Z = \infty$, using a parabolic fit $(a_1 + a_2 Z^{-1/3} + a_3 Z^{-2/3})$; see the red dashed line in Figure 1. In this calculation, we used accurate Kohn−Sham exact-exchange orbitals and densities.

The quantities E_x^{exact}/E_x^{LDA} and T_s^{exact}/T_s^{LDA} approximate the integrated average values of exact enhancement factors for exchange and kinetic energies, respectively. Thus, when their ratio approaches 1, we have a clear indication that the exchange and kinetic enhancement factors are very similar. Figure 1 thus shows how well the conjointness conjecture works for all of the noble gas atoms; for the He atom ($Z^{-1/3} = 0.79$), the ratio is in fact below 1.04, and for larger Z values, it is very close to unity, because quantum oscillations reduce for heavier atoms. At $Z = \infty$, the extrapolated ratio is about 0.997, whereas the *exact* ratio is 1,

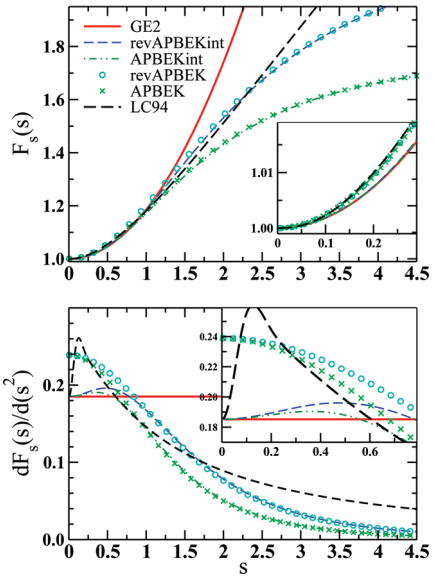

Figure 2. (Top panel) Kinetic energy enhancement factors and (lower panel) their derivative with respect to s^2. Note that $dF_s(s=0)/ds^2 = \mu_s$.

because LDA becomes exact in this limit for both exchange and kinetic energies.[77] These results indicate that the kinetic and exchange enhancement factors must be very similar on average, especially at small values of the reduced gradient s that dominate the core of heavy atoms.

2.3. PBE-Like Kinetic Functionals. We recently proposed[70] the APBEK (asymptotic PBE KE) GGA functional with the enhancement factor of eq 6 and $\mu_s = \mu_s^{MGE2} = 0.23889$. The value of κ_s^{APBEK} was fixed from a numerical analysis[70] of atoms with large Z to 0.804, i.e., like the one for the PBE exchange, despite no Lieb−Oxford bound holds for the KE. Thus, in APBEK, both μ_s and κ_s are nonempirical parameters, and it turned out that they are *very close to that of the TW02 functional, which was fitted to noble gas atoms.*

We also introduced the revAPBEK functional,[70] which is similar to the APBEK but with $\kappa_s^{revAPBEK} = \kappa_x^{revPBE} = 1.245$. In analogy with the revPBE exchange GGA functional, the revAPBEK functional takes advantage of the larger nonlocality granted by a higher value of κ_s and yields very accurate FDE energies.[70]

The APBEK and revAPBEK functionals satisfy several exact constraints of the KE but violate others.[50,55,78−82] In particular, they recover in the slowly varying density limit the MGE2 but not the GE2 expansion: within a simple GGA scheme, it is not possible to satisfy exactly both conditions. This situation resembles that of the exchange PBE functional, which yields μ_x^{PBE} and not μ_x^{GE2} for $s \to 0$. In this case, one possible solution was recently proposed by introducing the PBEint functional,[11] which correctly yields μ_x^{GE2} for small s while reproducing μ_x^{PBE} for slightly larger s (more important for atoms and molecules). Here, we follow a similar path and propose new KE GGA approximations (revAPBEKint and APBEKint) with the enhancement factor given by eq 6 and μ_s defined by

$$\mu_s^{int}(s) = \mu_s^{GE2} + (\mu_s^{MGE2} - \mu_s^{GE2}) \frac{\tau_s^W}{\tau_s^{HEG} + \tau_s^W} = \frac{3\mu_s^{GE2} + 5s^2\mu_s^{MGE2}}{3 + 5s^2} \quad (9)$$

where we used the von Weizsäcker kinetic energy density $\tau_s^W = \tau_s^{HEG} 5s^2/3$, and $\kappa_s^{APBEKint} = 0.804$ ($\kappa_s^{revAPBEKint} = 1.245$). We note that $\tau_s^{HEG} + \tau_s^W$ is the correct limit for a uniform density perturbed by a small-amplitude, short-wavelength density wave.[83]

In the upper panel of Figure 2, we report the enhancement factors of different KE functionals versus the reduced gradient s. In the lower panel of Figure 2, the derivatives of the enhancement factors with respect to s^2 versus the reduced gradient s are reported. Note that $dF_s(s=0)/ds^2 = \mu_s$.

For small s ($s < 0.5$), the APBEK and revAPBEK functionals have the behavior dictated by eq 7 and $F_s \rightarrow 1 + \mu_s^{MGE2} s^2$, thus recovering the MGE2 (in analogy with the APBE exchange functional[70]). On the other hand, by construction, both revAPBEKint and APBEKint KE functionals recover the correct GE2 for a slowly varying density. The LC94 functional recovers the correct GE2, but only at very small values of s ($s < 0.1$), as we can see in the lower panel of Figure 2. In the region $s < 0.5$, the enhancement factor of APBEK, revAPBEK, and LC94 cannot be distinguished; in a similar way, we have revAPBEKint ≈ APBEKint ≈ GE2. Significant differences are instead present in the lower panel of Figure 2. The LC94 functional displays a pronounced unphysical peak at small values of s, whereas the PBE-like functionals (APBEK and revAPBEK) have a smooth monotonic behavior. Two small peaks around $s = 0.5$ and $s = 0.4$ are observed for revAPBEKint and APBEKint, respectively.

In the range $0.5 < s < 2$, GE2 increases more rapidly than the other functionals. GE2 crosses the APBEK, revAPBEK, and LC94 curves at $s \approx 0.99$, 1.23, and 0.94, respectively.

For large s ($s > 2$), revAPBEK has a much larger enhancement factor than APBEK, as all the PBE-like functionals must approach the asymptotic value $1 + \kappa_s$. In this region, no differences can be observed between revAPBEK and revAPBEKint and between APBEK and APBEKint.

A totally different behavior is observed for LC94, which increases very rapidly for $s \geq 1$ but then decays asymptotically to zero as $s \rightarrow \infty$ (not shown in the figure). We note that this limit, where the density varies rapidly over a Fermi wavelength, is usually present only in evanescent regions such as the exponential decay of the density far in the tail. Several studies[2,3] pointed out that for atoms and molecules it is not energetically important, but it can be important to limit numerical errors.[84]

Finally, we calculate the c_1 and c_2 coefficients of eq 7 for different GGA approximations, using the same approach as in ref 76. All functionals that recover μ^{MGE2} give very accurate c_1 coefficients, whereas revAPBEKint, APBEKint, and GE2 yield larger deviations from the exact c_1, as expected (see Table 1). For the c_2 coefficient, a similar trend is found, but the agreement is not as good since the c_2 coefficient accounts for quantum oscillations that are not well described with gradient expansions. Notably, LC94 shows a good value for both c_1 and c_2, despite it formally recovering GE2 for $s \rightarrow 0$. This is due to the fact that *LC94 recovers GE2 only at very small values of s ($s \leq 0.1$), but in fact it is very close to the MGE2 behavior* over a wide range $0.1 \leq s \leq 1.2$.

Table 1. Deviations (Multiplied by 10^3) of c_1 and c_2 Coefficients, Computed for Different GGA Approximations, from Exact Ones (eq 7)[a]

	GE2	revAKi	AKi	revAK	AK	TW02	LC94
c_1	−36.2	−30.8	31.5	**−2.2**	−3.8	−8.0	−2.4
c_2	65.8	62.6	53.7	27.0	16.8	21.6	**7.2**

[a] The smallest values are in bold style. The following shorthands have been used for the functional names: AK for APBEK; revAK for revAPBEK; AKi for APBEKint; revAKi for revAPBEKint.

3. COMPUTATIONAL DETAILS

3.1. Atoms and Ions, Jellium Spheres, and Clusters. Densities and orbitals of atoms and ions (section 4.1) were obtained by analytic Hartree−Fock calculations.[85] For jellium clusters, we used accurate numerical exact exchange Kohn−Sham orbitals and densities,[86] for jellium surfaces, accurate numerical LDA Kohn−Sham orbitals and densities.[51]

3.2. FDE Calculations. The frozen density embedding calculations were performed within the KSCED formalism[25,32] with freeze-and-thaw cycles[87] to guarantee the full relaxation of the embedded ground-state electron densities: this approach is equivalent to Cortona's approach.[23] We used a development version of the TURBOMOLE program package.[88] Details of our FDE implementation in TURBOMOLE are discussed in ref 32. In the FDE calculations, the PBE[8] XC functional and def2-TZVPPD supermolecular basis set[89] were used. The def2-TZVPPD basis set adds diffuse basis functions to the def2-TZVPP[90] basis set and grants a very accurate description of weakly interacting systems. We used a very accurate integration grid (*gridsize* = 7, *radsize* = 14) to minimize numerical errors.

Several sets of molecular complexes with different kinds of interactions were considered in FDE calculations. The geometries of dispersion, dipole−dipole, and hydrogen bonding interacting systems were taken from the literature.[27,91,92]

The embedding error in the total energy was computed as

$$\Delta E = E^{FDE}[\tilde{\rho}_A^e, \tilde{\rho}_B^e] - E^{KS}[\rho^{KS}] \tag{10}$$

where $\tilde{\rho}_A^e(\mathbf{r})$ and $\tilde{\rho}_B^e(\mathbf{r})$ are the (approximated) embedded densities, E^{KS} is the total KS energy of total supermolecular system with density ρ^{KS}, and

$$\begin{aligned} E^{FDE}[\tilde{\rho}_A^e, \tilde{\rho}_B^e] = {} & T_s^{KS}[\tilde{\rho}_A^e] + T_s^{KS}[\tilde{\rho}_B^e] \\ & + \tilde{T}_s^{nadd}[\tilde{\rho}_A^e, \tilde{\rho}_B^e] + V_{ext}[\tilde{\rho}_A^e + \tilde{\rho}_B^e] \\ & + J[\tilde{\rho}_A^e + \tilde{\rho}_B^e] + E_{xc}[\tilde{\rho}_A^e + \tilde{\rho}_B^e] \end{aligned} \tag{11}$$

In eq 11, E_{xc} is the GGA exchange-correlation energy functional, J is the Coulomb energy, V_{ext} is the energy associated with the external potential, $T_s^{KS}[\tilde{\rho}_j^e]$ is the exact KS kinetic energy of the embedded subsystem j (actually computed from KS embedded *orbitals*), and finally the (approximated) nonadditive kinetic energy functional is

$$\tilde{T}_s^{nadd}[\tilde{\rho}_A^e, \tilde{\rho}_B^e] = \tilde{T}_s[\tilde{\rho}_A^e + \tilde{\rho}_B^e] - \tilde{T}_s[\tilde{\rho}_A^e] - \tilde{T}_s[\tilde{\rho}_B^e] \tag{12}$$

In this work, approximated functionals or densities are indicated with a tilde (˜). Equation 12 has two degrees of approximation: the functional form ($\tilde{T}_s$) and the embedded densities ($\tilde{\rho}_A^e$,$\tilde{\rho}_B^e$), which in turn depend on the approximated nonadditive kinetic energy potential.

A quantitative measurement of the absolute error associated with a given embedding density was obtained by computing the error

$$\xi = \frac{1000}{N} \int |(\tilde{\rho}_A^e(\mathbf{r}) + \tilde{\rho}_B^e(\mathbf{r})) - \rho^{KS}(\mathbf{r})| \, d\mathbf{r} \tag{13}$$

with N being the number of electrons. In evaluating ξ, we considered only the valence electron density (ξ_v): the core density

Table 2. Percent Mean Absolute Relative Error of Kinetic Energies of 51 Atoms and Ions (See Text), Jellium Surfaces (see ref 51) and Neutral Spherical Jellium Clusters (see refs 51 and 52)[a]

	GE2	revAKi	AKi	revAK	AK	TW02	LC94	ref.
atoms/ions	1.10	0.79	0.84	1.24	0.79	**0.72**	0.82	0.83[b]
surfaces	**3.30**	4.23	4.40	3.55	3.93	4.00	3.80	1.17,[c] 2.47,[d] 1.77[e]
clusters	0.99	1.02	1.14	**0.83**	0.96	0.98	0.92	1.76[c]
error	1.63	1.70	1.80	1.71	1.62	1.60	**1.59**	1.94[d]

[a] Also shown is the total error given by eq 20. Best (worst) results are indicated in boldface (underlined). The following shorthands have been used for the functional names: AK for APBEK; revAK for revAPBEK; AKi for APBEKint; revAKi for revAPBEKint. [b] The A0.185 functional from the Airy gas, see ref 52. [c] GE4 see ref 51. [d] MGGA kinetic functional, see ref 51. [e] The A(1/6) functional from the Airy gas, see ref 52.

is not important for the determination of chemical and physical properties of interaction between the subsystems.

3.3. Reduced Gradient Kinetic Energy Decomposition. To analyze the performance of different GGA kinetic functionals, we follow the idea proposed in ref 93, where the XC functional is decomposed in terms of its reduced gradient contributions, and apply it to kinetic energy functionals. Thus, we define the local (Thomas−Fermi) KE density in the s space

$$t[\rho](s) = \int \mathrm{d}\mathbf{r}\, \tau^{HEG}[\rho](\mathbf{r})\, \delta(s - s(\mathbf{r})) \tag{14}$$

so that

$$T_s^{HEG}[\rho] = \int \mathrm{d}s\, t[\rho](s) \tag{15}$$

We call $t[\rho](s)$ the *s-decomposed HEG kinetic energy distribution*. (Note that for a constant density, $t[\rho](s)$ becomes a Dirac function centered at $s = 0$.) For a GGA KE functional, we have

$$T_s^{GGA}[\rho] = \int \mathrm{d}\mathbf{r}\, \tau_s^{HEG}[\rho](\mathbf{r})\, F_s(s[\rho](\mathbf{r})) \tag{16}$$

and thus

$$T_s^{GGA}[\rho] = \int \mathrm{d}s\, t[\rho](s)\, F_s(s) \tag{17}$$

Equation 17 is very insightful: it states that the total kinetic energy is the scalar product (in the s space) of $t(s)$ and the kinetic enhancement factor $F_s(s)$.

A similar decomposition can also be obtained for the nonadditive kinetic energy (see eq 3). Hence,

$$T_s^{nadd}[\rho_A, \rho_B] = \int \mathrm{d}s\, t^{nadd}[\rho_A, \rho_B](s)\, F_s(s) \tag{18}$$

with

$$t^{nadd}[\rho_A, \rho_B](s) = t[\rho_A + \rho_B](s) - t[\rho_A](s) - t[\rho_B](s) \tag{19}$$

Equation 18 states that the nonadditive kinetic energy is the scalar product (in the s space) of the s-decomposed nonadditive HEG kinetic energy distribution $t^{nadd}(s)$ and the kinetic enhancement factor $F_s(s)$.

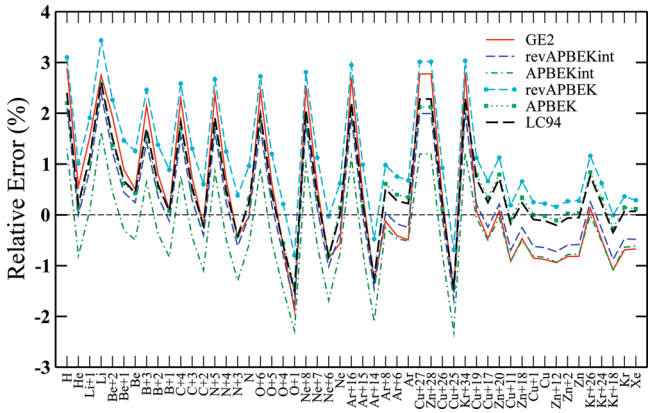

Figure 3. Percent mean absolute relative error for all atoms and ions considered, sorted by the exact kinetic energy.

In this paper, we present several plots of $t(s)$ and $t^{nadd}(s)$. These plots were obtained considering the values of the density and of the reduced gradient on a very accurate DFT quadrature grid.[94] To obtain a smooth curve, a Gaussian broadening in s (σ = 0.07) was used.

4. RESULTS

In this section, we present the results of the application of APBEK, revAPEK, revAPBEKint, and APBEKint functionals to different problems, ranging from the calculation of kinetic energies of atoms/ions and jellium clusters/surfaces to FDE calculations on many different complexes. For comparison, results obtained with the GE2, LC94, and TW02 functionals are also reported.

Molecular atomization kinetic energies have already been reported in ref 70. This test however leads to a very large absolute error for GGA KE functionals[51,52,95] and small differences among the PBE-like functionals.[70]

4.1. Atoms, Jellium Spheres, and Jellium Surfaces. In Table 2, we show the accuracy of different GGA functionals for the calculation of noninteracting kinetic energies of atoms/ions, jellium clusters, and jellium surfaces (similar to Table I of ref 51 and Table II of ref 52). The total error displayed in the last row of the table is defined as in refs 51 and 52.

$$Error = 100 \times \left(\frac{1}{2} MARE(atoms) + \frac{1}{4} MARE(clusters) + \frac{1}{4} MARE(LDM) \right) \tag{20}$$

where MARE(atoms) is the mean absolute relative error (MARE) of the integrated kinetic energy of 51 atoms and ions (listed in ref 51; in addition, we included Zn^{2+}, see Figure 3), MARE(clusters) considers neutral spherical jellium clusters with bulk parameter r_s = 3.93 (listed in ref 51), and MARE(LDM) is related to the jellium surface KE for r_s = 2, 4, and 6, calculated in the liquid drop model (LDM).[51]

Table 2 shows that the total error of eq 20 is practically the same for most of the functional approximations considered, because errors relative to different classes of systems compensate each other.

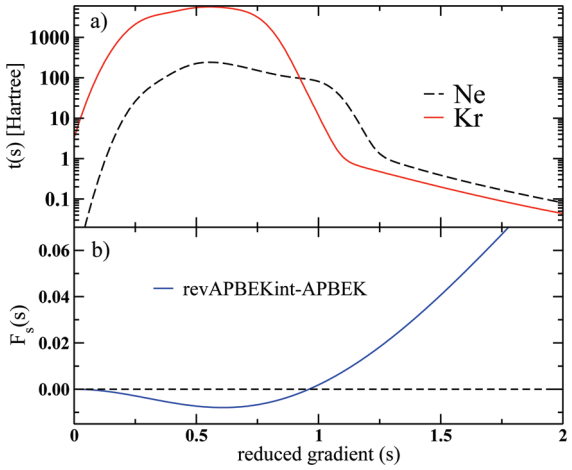

Figure 4. (Panel a) The *s*-decomposed HEG kinetic energy distribution $t(s)$ for Ne and Kr. (panel b) APBEK-revAPBEKint difference in the enhancement factor $F_s(s)$.

For atoms and ions, TW02 is the most accurate (MARE = 0.72), followed by APBEK, revAPBEKint, LC94, and APBEKint, all with similar errors (MARE = 0.79−0.82). We recall that TW02 and LC94 were fitted to atoms, in contrast to APBEKint and APBEK, which do not contain any empirical parameter. Instead, revAPBEK and GE2 show a lower accuracy. However, it is worth it to note that these functionals still outperform the fourth-order gradient expansion and meta-GGA functionals.[51]

To further investigate the errors in the kinetic energy for atoms and ions, in Figure 3, we report the relative error for all of the atoms and ions considered, sorted according to increasing (exact) kinetic energies.

Figure 3 shows that despite the MARE being below 1%, errors up to 3% can be present, in particular for small atoms and heavily charged ions. The relative error instead decreases for systems with a large number of electrons. In this case, the functionals recovering exactly or approximately μ_s^{MGE2} (i.e., APBEK, revAPBEK, TW02, LC94) are rather accurate, whereas those recovering μ_s^{GE2} (i.e., revAPBEKint, APBEKint) perform similar to the second-order gradient expansion and underestimate the kinetic energy. This can be easily seen by looking at the last two atoms (Kr and Xe) in Figure 3. This emphasizes the importance of the nonempirical parameter μ_s^{MGE2} for heavy atoms.

Note also that the total kinetic energy is always in the order revAPBEK > APBEK > revAPBEKint > APBEKint. While it can be easily expected that functionals with a larger κ_s or a large μ_s give larger kinetic energies (due to the larger enhancement factor), it is not obvious why APBEK > revAPBEKint, as the former has a larger μ_s while the latter has a larger κ_s. In addition, Figure 3 shows that the difference between these two functionals increases with the number of electrons: for Ne(Kr), the APBEK−revAPBEKint difference is 0.49% (0.61%).

To shine light on this issue, we report in Figure 4 (panel a) the *s*-decomposed HEG kinetic energy distribution $t(s)$ (see eq 14) and the difference of the two enhancement factors in panel b.

Figure 4a shows that the energy-relevant region for Ne is $0.2 < s < 1.3$: for larger *s*, $t(s)$ is vanishing exponentially (note that the energy axis is in a log scale). As the total kinetic energy can be obtained as the scalar product in the *s* space between $t(s)$ and $F_s(s)$, differences in $F_s(s)$ for $s < 1$ (where the revAPBEKint enhancement factor is lower than APBEK, due to a smaller μ_s parameter) are more important than differences due to different κ_s values (high *s* region). Upon increasing the atom size, the $t(s)$ distribution moves to smaller *s*, making the role of κ_s less important.

Coming back to Table 2, we see that for jellium surfaces, on the contrary, GE2 shows the best performance, although the error is quite large, because in this case a strong nonlocality is required and the fourth order-gradient expansion of the kinetic energy[96] needs to be recovered. In fact, laplacian-dependent functionals can be expected to perform accurately for these systems.[51] In addition, any GGA functional performing well for jellium surfaces will be rather inaccurate for atoms and molecules (see Figure 3 of ref 48). Because of the need for high nonlocality (i.e., large enhancement factor), better results are obtained with LC94, APBEK, and revAPBEK. Note also that the LC94 GGA has five empirical parameters fitted to the kinetic energies of He, He^+, Ne, and Ne^+ atoms.[64] Such a fitting set takes into account the ionization kinetic energy that contains a small contribution from atomic surface kinetic energy. Thus, for jellium surfaces, LC94 is favored with respect to the PBE-like GGAs.

Finally, for jellium clusters, which are in between surfaces and atoms, revAPBEK is the most accurate functional, while APBEK, TW02, and LC94 yield errors similar to GE2. Also, in this case, functionals with a higher κ_s are favored.

4.2. FDE Calculations. In this subsection, we present the results of FDE calculations on several sets of molecular complexes characterized by different types on nonbonded interactions:

WI weakly interacting systems (i.e., dispersion dominated). C_6H_6−Ne, $(CH_4)_2$, CH_4−Ne, He−Ne, Ar−Ne, and $(Ne)_2$, from the benchmark set WI7−05[91]

DI dipole interacting systems. CH_3Cl−HCl, CH_3SH−HCl, CH_3SH−NCH, $(H_2S)_2$, $(HCl)_2$, and H_2S−HCl, from the benchmark set DI6−04[92]

HB hydrogen-bonded systems. HF−NCH, a strong hydrogen-bond system deeply investigated in the context of the FDE theory;[27] $(H_2O)_2$, $(HCONH_2)_2$, $(HCOOH)_2$, $(HF)_2$, $(NH_3)_2$, and NH_3−H_2O from the benchmark set HB6-04[92]

Systems with a chemical bond and/or significant charge-transfer cannot be treated at the GGA level[38,39] and thus are not considered in this work. For these systems, corrections to GGA are required, as discussed in refs 82, 97, and 98.

4.2.1. Embedding Error on Energy. In Table 3, we report the embedding error on the total energy (ΔE), see eq 10. The KS binding energy (E_b^{KS}) of the total system is reported in the third column of Table 3. This was corrected for the basis-set superposition error (BSSE) using a counterpoise correction procedure,[99] and all geometries are kept fixed. Note that the embedding error on the total energy coincides with the embedding error of the binding energy, as the contributions from isolated subsystems cancel and, with a supermolecular basis set, the BSSE corrections also cancel. The results reported in Table 3 for the LC94 and TW02 functionals reproduce those reported in ref 38 and obtained with different basis sets. This shows the correct convergence of our calculations with respect to the basis set. The last column of Table 3 reports also the mean average error (MAE) for the LC94 and the LLP91[61] functionals from ref 38.

In each subgroup, the systems are sorted according to the reference E_b reported in the second column on the table. The E_b computed at the PBE level is in agreement with the reference values, since the PBE XC-functional correctly describes dipole−dipole and hydrogen-bond interactions.[92] On the other hand, PBE fails to describe correctly

Table 3. Energy Deviations between Supermolecular FDE and Kohn−Sham Calculations ($\Delta E = E^{FDE} - E^{KS} = E_b^{FDE} - E_b^{KS}$) Corresponding to Different KE GGA Functionals for Different Interactions (Weak, Dipole, Hydrogen-Bonded Systems)[a]

	E_b		$\Delta E = E^{FDE} - E^{KS} = E_b^{FDE} - E_b^{KS}$							
system	ref	E_b^{KS}	GE2	revAKi	AKi	revAK	AK	TW02	LC94	ref
					weak interaction					
He−Ne	0.06	0.14	−1.12	**0.08**	0.12	0.08	0.12	0.12	−0.10	
He−Ar	0.10	0.14	−1.17	**0.05**	0.10	0.05	0.10	0.09	−0.13	
$(Ne)_2$	0.13	0.18	−1.71	**0.12**	0.22	0.14	0.23	0.22	−0.15	
Ne−Ar	0.21	0.18	−1.90	0.10	0.22	**0.11**	0.24	0.22	−0.20	
CH_4−Ne	0.35	0.22	−2.13	0.10	0.24	**0.12**	0.26	0.24	−0.23	
C_6H_6−Ne	0.75	0.14[b]	−4.71	−0.08	0.40	**−0.03**	0.44	0.39	−0.73	
$(CH_4)_2$	0.81	0.02[b]	−4.49	−0.45	0.07	−0.38	0.13	**0.07**	−0.98	
MAE			2.46	0.14	0.20	**0.13**	0.22	0.19	0.36	0.35,[c] 0.14[d]
MARE (%)			831	**46**	83	49	88	81	98	88,[c,f] 29[d,f]
					dipole−dipole interaction					
$(H_2S)_2$	2.65	2.60	−4.99	−0.64	**0.28**	−0.48	0.44	0.34	−0.86	
$(HCl)_2$	3.20	3.06	−5.16	−0.12	0.97	**0.07**	1.15	1.03	−0.37	
H_2S−HCl	5.34	6.25	−5.62	0.12	1.57	0.40	1.85	1.70	**0.11**	
CH_3Cl−HCl	5.66	5.06	−7.77	−0.28	1.54	**0.02**	1.85	1.65	−0.45	
CH_3SH−HCN	5.72	5.39	−7.83	−1.41	−0.06	−1.18	0.16	**0.02**	−1.75	
CH_3SH−HCl	6.63	8.58	−7.54	**0.34**	2.47	0.73	2.87	2.66	0.48	
MAE			6.49	0.49	1.15	**0.48**	1.39	1.23	0.67	0.66,[c] 0.85[d]
MARE (%)			139	11.1	21.3	**9.6**	26.2	22.3	15.7	16,[c,f] 15[d,f]
					hydrogen bond					
$(NH_3)_2$	5.02	4.83	−6.68	−1.15	**0.04**	−0.95	0.24	**0.11**	−1.43	
$(HF)_2$	7.28	7.25	−6.43	0.54	2.05	0.79	2.29	2.12	**0.18**	
$(H_2O)_2$	7.92	7.83	−7.35	−0.47	1.13	**−0.20**	1.40	1.23	−0.69	
NH_3−H_2O	10.21	10.81	−7.91	−0.76	1.08	**−0.44**	1.41	1.22	−0.77	
HF−NCH	11.33	12.32	−8.05	0.07	2.18	0.43	2.55	2.33	0.09	
$(HCONH_2)_2$	23.81	23.34	−19.36	−4.94	−0.75	−4.20	**0.02**	−0.41	−4.52	
$(HCOOH)_2$	25.74	28.08	−18.95	−2.74	2.34	−1.87	3.29	2.80	**−1.71**	
MAE			10.67	1.53	1.37	**1.27**	1.60	1.46	1.34	1.44,[c,e] 1.07[d,e]
MARE (%)			87.1	10.9	11.8	**9.3**	14.3	12.7	10.6	11,[c,e,f] 9[d,e,f]
					all systems					
MAE			6.54	0.73	0.89	**0.63**	1.05	0.95	0.80	
rwMAE			9.05	0.78	1.08	**0.70**	1.26	1.13	1.17	
rwMARE			8.75	0.72	1.10	**0.66**	1.29	1.14	1.03	

[a] The first two columns report the binding energy (E_b) from reference data[91] and from Kohn−Sham calculations with the PBE XC functional (E_b^{KS}). The mean absolute error (MAE) and the mean absolute relative error (MARE) are also shown for each set of molecules. In the last row, the relative weighted MAE (rwMAE) and the global relative weighted MARE (rwMARE) are reported. Bold style indicates the smallest error in each row. All energies are in mHa (1mHa = 0.62751 kcal/mol). The following shorthands have been used for the functional names: AK for APBEK; revAK for revAPBEK; AKi for APBEKint; revAKi for revAPBEKint. [b] E_b^{KS} differs significantly from the reference value, and it is very small. Thus, to compute the MARE, we use (in the denominator) the reference value of E_b. [c] LC94 functional, see ref 38. [d] LLP91 functional, see ref 38. [e] Without HF-NCH. [f] Recomputed from data in ref 38.

systems with significant dispersion interaction (see e.g. C_6H_6−Ne and $(CH_4)_2$), although for other systems the PBE functional can capture the short-range part of the dispersion interaction.

To compare results from different classes of systems, and have a global indicator for the performance of the different KE functionals, we consider the relative weighted MAE (rwMAE) among all of the subgroups, namely

$$rwMAE = \frac{1}{3}\sum_{i=WI,DI,HB}\left(\frac{MAE_i}{\langle MAE_i\rangle}\right) \quad (21)$$

where $\langle MAE_i\rangle$ is the average MAE among all of the different functionals (but GE2) for subgroup i (we used two-digit accuracy, thus $\langle MAE_{WI}\rangle = 0.2$, $\langle MAE_{DI}\rangle = 0.9$, $\langle MAE_{HB}\rangle = 1.4$). In this way, all of the different subgroups have the same mean influence on the rwMAE, and functionals with rwMAE larger (smaller) than 1 have a worse (better) performance than the average.

Alternatively, we also consider the mean absolute relative error (MARE) of ΔE relative to the E_b computed at the supermolecular PBE level. In this way, large absolute differences between systems with different sizes are eliminated, and a better

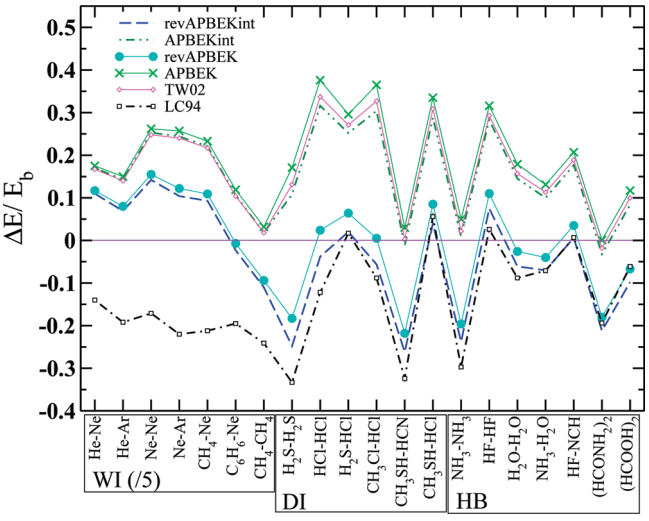

Figure 5. Relative embedding energy error ($\Delta E/E_b$) for all of the systems investigated. $\Delta E = E^{FDE} - E^{KS}$. E^{KS} is the total energy from supermolecular Kohn−Sham PBE calculations. E_b is the PBE Kohn−Sham binding energy, but for C_6H_6−Ne and $(CH_4)_2$ where the reference binding energy[91] was considered. For graphical reasons, the errors of the first seven systems (WI) have been divided by a factor of 5.

comparison is possible. However, for the systems C_6H_6−Ne and $(CH_4)_2$, the E_b at the PBE level is very small, so that the MARE will almost diverge. For these two systems, we thus considered the error relative to the reference E_b (second column of Table 3). In any case, the accuracy of the MARE for the WI system is not very significant, and for this reason, we report in Table 3 only two digits. The relative error ($\Delta E/E_b$) for all systems is shown in Figure 5, where the error for WI systems was divided by a factor of 5.

Finally, we consider a global relative weighted error (rwMARE) defined as

$$rwMARE = \frac{1}{3}\sum_{i=WI,DI,HB}\left(\frac{MARE_i}{\langle MARE_i\rangle}\right) \quad (22)$$

with $\langle MARE_{WI}\rangle = 74$, $\langle MARE_{DI}\rangle = 18$, and $\langle MARE_{HB}\rangle = 12$.

Considering the MAE for all systems, we have, first of all, to emphasize that these errors are as small (0.6−1.0 mHa) as the errors due to the approximated XC functionals.[92] This means that the FDE method can be successfully used to describe these systems. The revAPBEK functional yields the best overall results with a MAE of 0.63 mHa, outperforming the LC94 (and TW02) results. More importantly, the rwMAE (rwMARE) of revAPBEK is by 40% (36%) smaller than that of LC94.

On the other hand, the APBEK functional shows the worst overall performance. However, we must recall that the APBEK has *no empirical parameters* and was designed to recover the correct kinetic energy of atoms with an infinite number of electrons, whereas here we are considering small systems in the first two rows of the periodic table. Indeed, the APBEK functional has a global performance similar to that of the TW02 functional, which contains two empirical parameters. TW02 is slightly better due to the somehow larger κ_s value. The comparison between APBEK, TW02, and revAPBEK in fact clearly shows that a large value of κ_s is needed to obtain improved embedding energies.

For DI systems, functionals with a high enhancement factor in the large *s* region (i.e., revAPBEKint, revAPBEK and LC94) show a much better performance (with a MAE/MARE 2−3 times smaller) than functionals with a small κ_s (i.e., APBEK and TW02). The revAPBEK functional has a MAE/MARE which is 40% better than the LC94 one. The very good performance of revAPBEK can also be inspected in Figure 5: APBEK and TW02 largely overestimate ΔE, and LC94 underestimates it, while revAPBEK is in between them with a MARE of only 9%.

Larger κ_s values also improve ΔE for WI systems, but with a smaller ratio (less than a factor of 2). For these systems, LC94 seems to have a too large enhancement factor, as it yields largely underestimated energies (see Figure 5) with a MAE = 0.36 mHa. The MAE of the revAPBEK is almost 3 times smaller than that of the LC94 functional and revAPBEK shows a similar performance to that of the LLP91 functional, which is the most accurate one for this benchmark.[38]

For HB systems, the role of κ_s is further reduced, and differences among functionals are smaller. Figure 5 shows that for HB systems all of the functionals give almost exactly the same profile, except for a constant shift. The APBEK (revAPBEK) is the best (the worst) for $(HCONH_2)_2$ and $(NH_3)_2$. Considering all HB systems, the revAPBEK functional gives the best MAE and the same MARE as the LLP91 functional.

It is worth it to note that revAPBEK also gives the same MARE (9%) for both DI and HB, meaning that it can provide a balanced description of all kinds of interactions.

Concerning the other important limit, i.e., the one for small *s*, the revAPBEKint functional (which recovers GE2 at small *s*) is, considering all systems, also much better than LC94/TW02, but it is slightly worse than revAPBEK (rwMAE/rwMARE 0.08/0.06 higher). This is more evident for the HB systems. On the other hand, APBEKint is better than APBEK (rwMAE/rwMARE 0.16/0.19 smaller). This shows that there is an inter-relation between the large- and small-*s* regimes and that *both the MGE2 limit for μ_s and the large κ_s value are required to obtain a very good performance.* Finally, we note that ΔE values are always in the order APBEK > APBEKint > revAPBEK > revAPBEKint, see Table 3 and Figure 5. This order is different from that observed for atoms. We will come back to this important issue in section 5.

4.2.2. Embedding Error on Density. To further analyze the ability of different KE functionals to yield accurate nonadditive kinetic energy potentials, we inspected the errors in embedding densities (see eq 13) and reported them in Table 4. The analysis of the deformation densities is frequently employed to assess the approximations made within the FDE scheme.[32,100−103] In fact, while the analysis of interaction energies can be affected by error-compensation between approximated kinetic energy functionals and approximated embedding densities, the errors on the embedding densities give a direct benchmark of the quality of the kinetic energy potential.

The last two rows of Table 4 report the MAE for all systems and the rwMAE, computed as in eq 21. These data show that *all* functionals yield very accurate densities. GE2 fails for the WI systems (as it excessively favors charge-transfer and covalent bonding), but it is instead quite accurate for HB and DI ones.

Functionals with a high enhancement factor in the large-*s* region (i.e., revAPBEKint, revAPBEK and LC94) show a slightly worse performance than the ones with small κ_s (i.e., APBEK, APBEKint, and TW02), but the differences in the global MAE are very small (less than 5%). On the other hand, differences between different μ_s values can be hardly distinguished.

Table 4. Global Absolute Errors on Valence Embedding Density ξ_v (See eq 13) Resulting from Supermolecular FDE Calculations with Different KE Functionals on Different Classes of Systems (Weak, Dipole, Hydrogen-Bonded Systems)[a]

system	GE2	revAKi	AKi	revAK	AK	TW02	LC94
			weak interaction				
He−Ne	0.60	**0.04**	0.08	0.05	0.09	0.08	0.10
He−Ar	0.79	**0.06**	0.07	**0.06**	0.07	0.07	0.17
$(Ne)_2$	0.50	**0.03**	0.09	0.04	0.09	0.09	0.08
Ne−Ar	0.64	**0.06**	0.10	**0.06**	0.11	0.10	0.12
CH_4−Ne	0.77	**0.07**	0.10	**0.07**	0.11	0.10	0.14
C_6H_6−Ne	0.70	0.15	**0.08**	0.13	0.09	**0.08**	0.17
$(CH_4)_2$	1.45	0.65	0.35	0.61	**0.31**	0.34	0.59
MAE	0.78	0.15	**0.12**	0.15	**0.12**	**0.12**	0.20
			dipole−dipole interaction				
$(H_2S)_2$	2.18	1.88	**1.75**	1.86	1.76	1.76	1.80
$(HCl)_2$	2.00	1.88	**1.85**	1.89	1.87	1.87	1.92
H_2S−HCl	**3.50**	3.70	3.73	3.74	3.78	3.77	3.75
CH_3Cl−HCl	2.53	2.40	**2.33**	2.40	2.35	2.35	2.40
CH_3SH−HCN	2.03	1.75	1.57	1.72	**1.54**	1.55	1.61
CH_3SH−HCl	**3.95**	4.11	4.11	4.15	4.15	4.15	4.13
MAE	2.70	2.62	**2.56**	2.63	2.58	2.58	2.60
			hydrogen bond				
$(NH_3)_2$	2.20	1.83	1.60	1.79	**1.58**	1.59	1.69
$(HF)_2$	1.76	**1.54**	**1.54**	1.55	1.57	1.57	1.64
$(H_2O)_2$	2.25	2.04	**1.95**	2.03	1.96	1.97	2.04
NH_3−H_2O	3.12	3.14	**3.07**	3.14	3.08	3.08	3.07
HF−HCN	**2.66**	2.84	2.81	2.84	2.82	2.82	2.79
$(HCONH_2)_2$	2.78	2.79	2.60	2.76	**2.57**	2.58	2.59
$(HCOOH)_2$	3.39	3.47	**3.38**	3.47	**3.38**	3.39	3.39
MAE	2.59	2.52	**2.42**	2.51	**2.42**	2.43	2.46
			all				
MAE	1.99	1.72	**1.66**	1.72	**1.66**	1.67	1.71
rwMAE	2.55	1.04	**0.95**	1.03	0.96	**0.95**	1.13

[a] The mean absolute error (MAE) for each set of molecules and, in the last row, the rwMAE for these weakly-bonded systems are also reported. Bold style indicates the smallest error in each row. The following shorthands have been used for the functional names: AK for APBEK; revAK for revAPBEK; AKi for APBEKint; revAKi for revAPBEKint.

These small modifications in the description of the density indicate that all functionals yield a reasonably good kinetic energy potential, and we can suppose that the corresponding density differences will therefore play a minor role in the determination of errors on embedding energies (see section 5).

In addition, we found that the embedding errors in the density have similar spatial distribution. This can be inspected from Figures S1−S4 of the Supporting Information, where we reported the plane averaged absolute error in the embedded valence density, i.e. $\int\int dx\, dy\, |\rho_{val}^{FDE}(\mathbf{r}) - \rho_{val}^{KS}(\mathbf{r})|$, where z is the interaction axis, for different systems.

5. DISCUSSION

For the exact T_s^{nadd}, the embedded density will be exact (i.e., the sum $\rho_A^e(\mathbf{r}) + \rho_B^e(\mathbf{r})$ will yield the total KS density of the total system $\rho^{KS}(\mathbf{r})$) and $\Delta E = 0$. For an approximate $\tilde{T}_s^{nadd}$, we have instead

$$\Delta E[\tilde{\rho}_A^e, \tilde{\rho}_B^e] = \tilde{T}_s^{nadd}[\tilde{\rho}_A^e, \tilde{\rho}_B^e] + \Delta W[\tilde{\rho}_A^e, \tilde{\rho}_B^e] \tag{23}$$

where

$$\begin{aligned}\Delta W[\tilde{\rho}_A^e, \tilde{\rho}_B^e] = {} & T_s^{KS}[\tilde{\rho}_A^e] + T_s^{KS}[\tilde{\rho}_B^e] - T_s^{KS}[\rho^{KS}] \\ & + V_{ext}[\tilde{\rho}_A^e + \tilde{\rho}_B^e] - V_{ext}[\rho^{KS}] \\ & + J[\tilde{\rho}_A^e + \tilde{\rho}_B^e] - J[\rho^{KS}] \\ & + E_{xc}[\tilde{\rho}_A^e + \tilde{\rho}_B^e] - E_{xc}[\rho^{KS}]\end{aligned} \tag{24}$$

The subdivision in eq 23 is interesting because ΔW depends *only* on the approximation for the nonadditive kinetic *potential*, as it depends only on the embedded densities. In other words, ΔW is a *known* bifunctional of the embedded densities.

If we consider a set of KE functionals which yield very similar embedding densities (as is the case for the PBE-like ones considered in this work), then for any given enhancement factor $F_s(s)$ in this set, ΔW can be approximately considered independent of $F_s(s)$ (i.e., it is a constant) and

$$\begin{aligned}\Delta E[F_s] &\approx \tilde{T}_s^{nadd}[F_s] + \Delta W \\ &\approx \int ds\, t^{nadd}(s)\, F_s(s) + \Delta W\end{aligned} \tag{25}$$

where we used eq 18. Equation 25 means that differences in ΔE among different KE functionals are *directly related to differences in the enhancement factor* $F_s(s)$ for the kinetic energy, if embedding densities are not changing.

In order to verify the validity of eq 25 for the systems and the functionals under investigation in this work, we consider the relation between the following two quantities:

$$\begin{aligned}e[F_s] &= \frac{\Delta E[F_s] - \Delta E[F_s^{APBEK}]}{\Delta T} \\ t[F_s] &= \frac{\tilde{T}_s^{nadd}[F_s] - \tilde{T}_s^{nadd}[F_s^{APBEK}]}{\Delta T}\end{aligned} \tag{26}$$

where

$$\Delta T = \max_{F_s}\{\tilde{T}_s^{nadd}\} - \min_{F_s}\{\tilde{T}_s^{nadd}\} \tag{27}$$

is used to normalize the range of variation of the nonadditive kinetic energies. With the above definitions, $e[F_s^{APBEK}] = t[F_s^{APBEK}] = 0$ (to set a reference value), $e[F_s] < e[F_s^{APBEK}]$ (as we found that APBEK gives the highest ΔE, see Figure 5), and $t[F_s] > -1$. If eq 25 holds exactly, then a plot of $e[F_s]$ against $t[F_s]$ gives a straight line with a slope of -1. Tables with all values of T_s^{nadd} and ΔW are reported in the Supporting Information.

In Figure 6, we consider four functionals in the order APBEK, APBEKint, revAPBEK, and revAPBEKint and all of the systems considered in this work. Figure 6 clearly shows that, (i) for all of the WI and HB systems, eq 25 holds almost exactly and, (ii) for DI systems, a different behavior is found: in particular (rev)APBEKint has a larger $\tilde{T}_s^{nadd}$ than (rev)APBEK.

In order to shine light on these two findings, we report in Figure 7 the s-decomposed nonadditive HEG kinetic energy distribution $t^{nadd}(s)$ (considering LC94 embedded densities) for four representative systems.

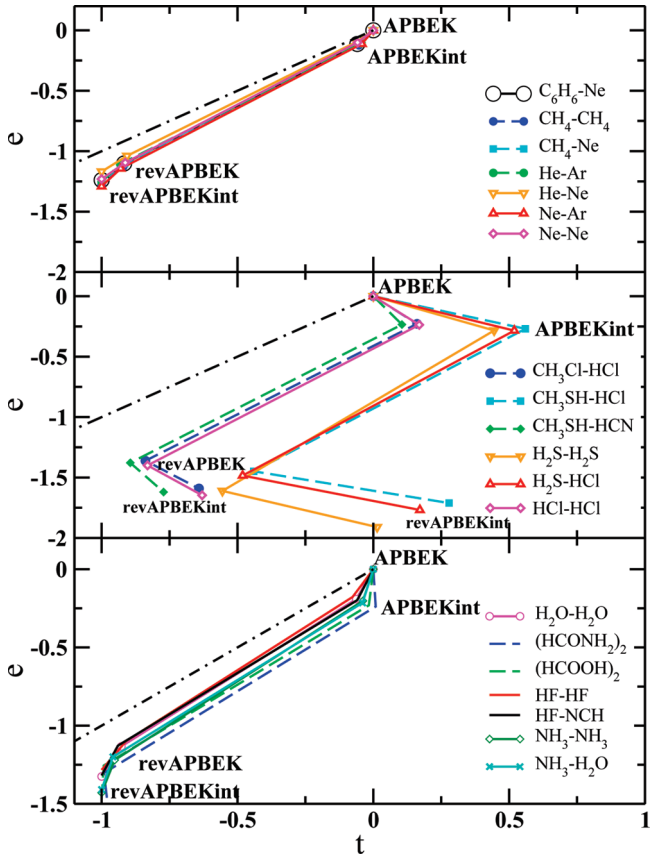

Figure 6. Relation between $e[F_s]$ and $t[F_s]$ (see text for definitions) for weakly interacting systems (panel a), dipole-interacting systems (panel b), and hydrogen-bonded systems (panel c). The values at $e = t = 0$ represent the (reference) APBEK results. Lines starting from it show the values for the APBEKint, revAPBEK, and revAPBEKint functionals (in this order). In each panel, the black dot-dashed line with slope −1 represents the ideal behavior according to eq 25.

Figure 7 shows that upon formation of a bond, there is a decrease of kinetic-energy density at large s (i.e., in the tail of the isolated molecules) and an increase at small s (i.e., in the bond region). The sign change of $t^{\mathrm{nadd}}(s)$ occurs at about $s = 1.2-1.3$ for both DI and HB systems, and only the region with $s < 3$ is energetically important. For the WI system, the sign change happens at a larger s, due to the large intermolecular equilibrium distances. The alternating behavior of $t^{\mathrm{nadd}}(s)$ for the systems illustrated in Figure 7 directly explains the differences in ΔE and $\tilde{T}_s^{\mathrm{nadd}}$ among different functionals (see eq 18). In fact:

- KE functionals with a large enhancement factor at large s (revAPBEK and revAPBEKint) have *lower* ΔE and $\tilde{T}_s^{\mathrm{nadd}}$ than the corresponding ones with smaller k_s (APBEK and APBEKint), because $t^{\mathrm{nadd}}(s)$ is *negative* at large s.
- In a similar way, KE functionals with a higher enhancement factor at small s (APBEK and revAPBEK) have *higher* ΔE and $\tilde{T}_s^{\mathrm{nadd}}$ than the corresponding ones with smaller μ_s (APBEKint and revAPBEKint), because $t^{\mathrm{nadd}}(s)$ is *positive* at small s.

These findings rationalize the performance of different functionals. We discuss hereafter in more detail one representative example for the case where eq 25 holds, the water dimer. For this system, revAPBEK has a ΔE of only −0.2 mHa, whereas APBEK is much worse (ΔE = 1.4 mHa). The

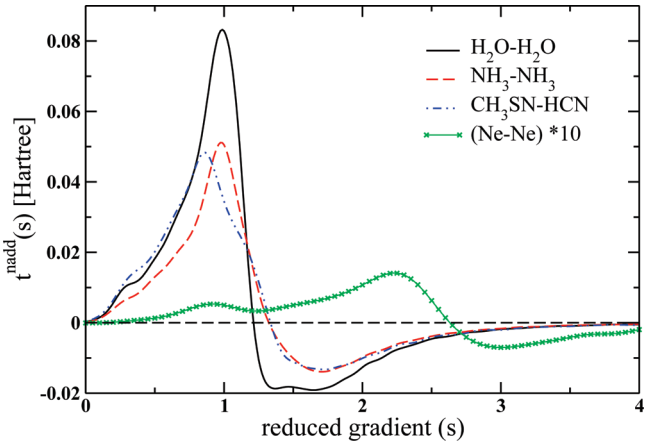

Figure 7. s-Decomposed nonadditive HEG kinetic energy density distribution t^{nadd} for H_2O-H_2O, NH_3-NH_3, $CH_3SH-HCN$, and $(Ne)_2$ (the latter is multiplied by a factor of 10 for graphical reasons).

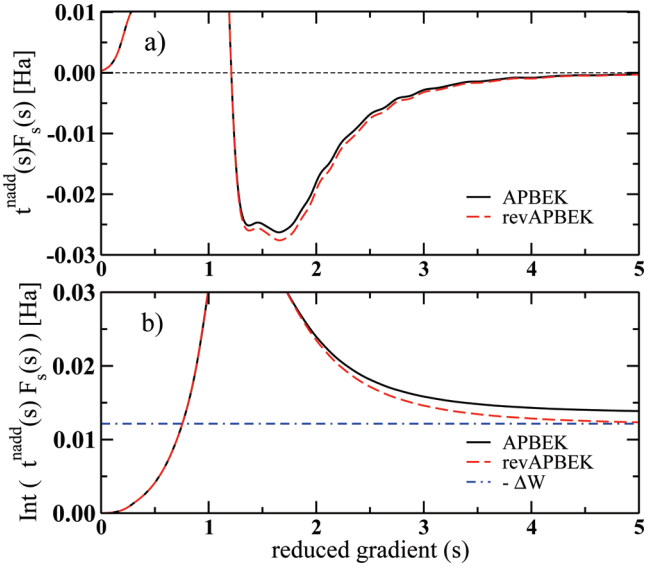

Figure 8. Contributions to the nonadditive kinetic energy for H_2O-H_2O, using the APBEK and the revAPBEK functionals, fixing the embedded density to the APBEK ones. (Panel a) The s-decomposed nonadditive HEG KE distribution t^{nadd} multiplied by the enhancement factor ($F_s(s)$) as a function of the reduced gradient (s). (Panel b) Cumulative integral of the data in panel a. Also shown, the $-\Delta W$ value (from APBEK).

corresponding values of ΔW are −12.44 and −12.15 mHa, respectively (see Supporting Information): thus differences in the embedded densities are negligible with respect to differences in $\tilde{T}_s^{\mathrm{nadd}}$. We thus fix the density to the APBEK one, and in Figure 8, we plot $t^{\mathrm{nadd}}(s)\,F_s(s)$ (panel a) and $\int_0^s t^{\mathrm{nadd}}(s')\,F_s(s')\,ds'$ (panel b).

The plots clearly show that differences are significant only for $s >$ 1.5. For this reason, if we define the *correct* value of the approximated $\tilde{T}_s^{\mathrm{nadd}}$ as the one that gives $\Delta E = 0$, i.e., $\tilde{T}_s^{\mathrm{nadd}} = -\Delta W$, we note that the larger $F_s(s)$ at high s of the revAPBEK reduces the $\tilde{T}_s^{\mathrm{nadd}}$ energy toward the correct value. Clearly, this condition holds due to an error cancellation. In fact, for a given system, different approximate KE functionals (i.e., different enhancement factors) might exists which satisfy $\tilde{T}_s^{\mathrm{nadd}} = -\Delta W$, although both

$\tilde{T}_s^{nadd}$ and ΔW can be significantly different from the ones obtained with the exact KE functional. Actually, accurate KE functionals should reproduce the *exact* T_s^{nadd} and ΔW *separately*, and not only their sum. However, these *exact* values cannot be easily obtained because they will require in practice the solution of an inverse-KS problem,[104,105] in order to obtain the exact nonadditive kinetic potential and the exact embedded density.[33,103,106−108] Nevertheless, within a simple (and efficient) GGA approach, we can consider a KE functional to be accurate for FDE applications if it can obtain a good performance over a very large set of systems, i.e., achieving similar error cancellation for different systems. Indeed, as shown in Table 3, the larger κ_s value of the revAPBEK functional improves ΔE for the largest number of systems and yields the best averaged performance (rwMARE = 0.66).

Clearly, a different empirically optimized value κ_s may also be found that yields even a better performance for the FDE energies for a given set of systems. To demonstrate our latest statement, we note that (see Figure 5) for HB systems all of the functionals give the same profile, with only a constant shift. This means that none of the considered PBE functional forms can achieve in this case a vanishing error for all of the HB systems, but further tuning of the κ_s value can then be used to reduce the MAE. In fact, we recomputed all seven HB systems for $\kappa_s = 1$ (and $\mu_s = \mu_s^{MGE2}$), and we found a MAE of 1.050 mHa, i.e., almost the same as that of the LLP91 functional, which yields the lowest MAE among different KE functionals considered in ref 38. We note however that with $\kappa_s = 1$ the description of $(NH_3)_2$, $(HCOOH)_2$, and $(HCONH_2)_2$ is improved (with respect to revAPBEK), but for other systems, the energy is overestimated (see Supporting Information). Furthermore, we found that the MARE is not reduced (still 9%) with respect to revAPBEK. It is worth it to recall that in the revAPBEK functional the κ_s value was chosen without taking into account weakly bounded systems but just following the conjointness relation with the improved exchange energy of the revPBE functional.[72] In this sense, the revAPBEK functional can also be considered *nonempirical*.

On the other hand, Table 3 and Figure 5 show that a modification of the enhancement factor for small s (i.e., a reduction of the μ_s parameter) does not lead to large differences in the embedding energies, as $t^{nadd}(s)$ is very small in this region. However, revAPBEKint (rwMARE = 0.72) is even less accurate than revAPBEK (rwMARE = 0.66), mainly due to the worse description of HB systems. Thus, functionals which satify the MGE2 limit provide *both* accurate embedding energies and accurate total KE, where, see Figure 4, the important region is $s < 1.3$. The improvement of APBEKint (rwMARE = 1.10) with respect to APBEK (rwMARE = 1.29) for embedding energies can be instead traced back to an error-compensation for the too small κ_s. In fact, $\tilde{T}_s^{nadd}$ can be reduced by decreasing μ_s or increasing κ_s. However, APBEKint is the worst functional for the benchmark in Table 2.

Coming back to Figure 6, we now discuss the DI systems, where eq 25 does not hold. First of all, we note that the APBEKint and revAPBEKint functionals lead to larger T_s^{nadd} values but lower ΔE values than APBEK and revAPBEK, respectively. This traces back to a significant reduction of ΔW from (rev)APBEK to (rev)APBEKint KE functionals (see Supporting Information), originating from relatively large variations of the embedded density. To better understand this point, we plot in Figure 9 the difference of t^{nadd} calculated at the APBEKint and APBEK levels (both different enhancement factors and densities were used here).

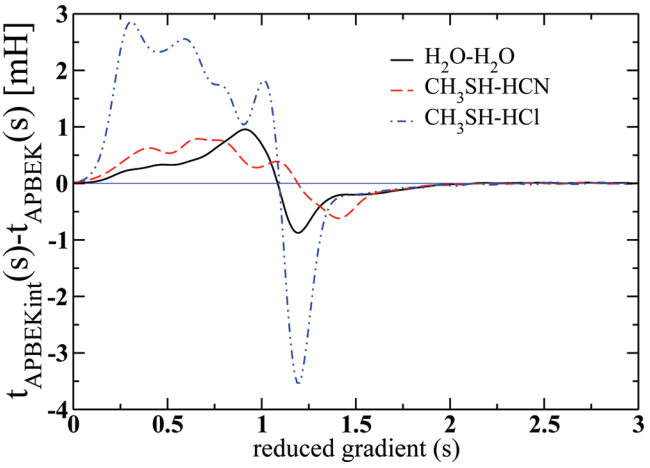

Figure 9. Difference in the s-decomposed nonadditive HEG kinetic energy density distribution, between the APBEKint and APBEK functionals, for H_2O-H_2O, $CH_3SH-HCN$, and $CH_3SH-HCl$.

The figure clearly shows that for $CH_3SH-HCl$ the kinetic energy density at small s values is much larger for APBEKint than for APBEK, which accounts for the large T_s^{nadd} variation (see Figure 6b). A similar effect is also present for $CH_3SH-HCN$, with lower intensity, while for the H_2O dimer only a small oscillation, with opposite peaks of equal intensity, is found, so that upon integration the difference between APBEKint and APBEK is averaged out (T_s^{nadd} changes by 0.1 mHa from APBEKint and APBEK, see Supporting Information). The higher kinetic energy density at small s observed for APBEKint indicates that a higher electron density is present in the bonding region when this functional is used. The reason for this is probably relayed in the behavior of the APBEKint enhancement factor at small s (recovering $1 + \mu^{GE2}s^2$), which favors delocalization of the density in the bond. This effect is larger for the DI systems because they contain highly polarizable atoms of the second row (S, Cl).We note finally that an increased density in the bond region is a small effect and does not necessarily correlate with improvements in the embedded density (see Table 4).

6. SUMMARY AND CONCLUSIONS

In this paper, we have reviewed the recently introduced APBEK and revAPBEK GGA kinetic energy functionals and have presented an extended study of their ability to compute kinetic energies of atoms and jellium clusters and surfaces and their performance in supermolecular FDE calculations.

These nonempirical functionals recover the MGE2 expansion and have been constructed mainly from the semiclassical theory of the many-electron neutral atoms, which incorporates a strong conjointness conjecture, as we showed in Figure 1. However, small perturbations of the homogeneous electron gas are correctly described by the second-order gradient expansion (GE2), and due to the simplicity of the GGA level, any semilocal functional cannot recover both expansions in the slowly varying density limit. Thus, we introduced two new functionals, APBEKint and revAPBEKint, which recover the GE2 limit at small s and which have enhancement factors similar to the PBEint exchange functional of ref 11.

The APBEK and revAPBEK functionals show performances comparable and in many cases superior to the current state-of-the-art for GGA KE functionals, which in this context were represented by functionals such as LC94 and TW02. The

accuracy of these latter two functionals relied on empirical parametrization to the kinetic energy of small atoms: we showed instead that this empirical parametrization led to enhancement factors which closely resemble the MGE2. This means that the MGE2 (exact for an atom with a large number of electrons) is very accurate also for small atoms so that the MGE2 represents a new paradigm for the construction of accurate and nonempirical kinetic energy functionals.

However, the MGE2 mainly defines the behavior of the enhancement factor for small values of the reduced density gradient, and furthermore GGA KE functionals are approximations of integrated KE T_s and not of KE density τ. Thus, GGA KE functionals rely on error cancellation. To shine light on the role of gradient corrections in KE functionals, we have introduced the *s* decomposition of KE, equivalent with the KE distribution in the *s* space (see eqs 14−19). Our approach can well show the behavior of a GGA for a given system (see Figures 4, 6, 7−9) and can be a useful tool in the FDE and kinetic energy development fields.

Our analysis showed that the performance of PBE-like functionals depends on a balance between the low and high *s* region: thus, for accurate results, μ_s and κ_s must be interrelated. Results presented in this work show that functionals which satisfy the exact MGE2 limit have to be preferred. In fact:

- For the total kinetic energy in atoms/ions and in jellium clusters/surfaces, APBEK performs best and its accuracy increases for large atoms; in these cases, revAPBEK is also accurate, while functionals that satisfy the GE2 limit strongly underestimate the kinetic energy.
- For a benchmark of 20 small molecules with dispersion, dipole−dipole, and hydrogen bond interactions (thus incorporating the behavior of a very large set of molecular systems), we have found that revAPBEK is the most accurate functional for FDE interaction energies (see Table 3), while all of the PBE-like functionals give similar (small) integrated embedding density errors (see Table 4). Recovering the GE2 does not lead to improved accuracy. The similarity of the embedding errors on the density and their similar spatial distribution (see Figures S1−S4 in the Supporting Information) suggests that all of the nonadditive kinetic energy potentials are rather similar.

Therefore, the revAPBEK GGA functional can be considered as the current best choice for FDE calculations of nonbonded systems, because it is nonempirical and it has a well balanced accuracy for any kind of weak interaction.

Our embedding energy *s* decomposition (eq 25) shows that the performance of the GGA KE functional might be still be improved. In fact, it should be possible to develop new enhancement factors[109] eventually with the inclusion of the laplacian of the density,[51,53,80,109] which can improve the accuracy of the energy without changing the embedded density. In this context, the MGE2 is an important limit to be satisfied to reduce empiricism.

Future works should also verify the accuracy of the revAPBEK functional for the embedding energy of large systems containing heavy atoms, where the MGE2 limit is expected to work better. Furthermore, error cancellation can also occur with the approximate XC functional. In this work, we used PBE, but the new APBE XC functional[70] might be more appropriate.

■ ASSOCIATED CONTENT

Ⓢ Supporting Information. Tables containing $\tilde{T}_s^{\mathrm{nadd}}[\tilde{\rho}_A^e,\tilde{\rho}_A^e]$ and $\Delta W[\tilde{\rho}_A^e,\tilde{\rho}_A^e]$ for all systems and functionals; a table of embedding errors for hydrogen bond systems, using a revAPBEK kinetic energy functional with κ_s = 1.0; figures on the plane averaged absolute error on the embedded valence density for various systems. This information is available free of charge via the Internet at http://pubs.acs.org/.

■ AUTHOR INFORMATION

Corresponding Author
*E-mail: fabio.dellasala@unisalento.it.

■ ACKNOWLEDGMENT

We thank TURBOMOLE GmbH for providing us the TURBOMOLE program package and M. Margarito for technical support. This work was funded by the ERC Starting Grant FP7 Project DEDOM, Grant Agreement No. 207441.

■ REFERENCES

(1) Kohn, W.; Sham, L. *Phys. Rev.* **1965**, *140*, A1133.
(2) Parr, R. G.; Yang, W. *Density-Functional Theory of Atoms and Molecules*; Oxford University Press: Oxford, 1989; pp 1− 333.
(3) Dreizler, R. M.; Gross, E. K. U. *Density Functional Theory*; Springer: Heidelberg, 1990; pp 1−302.
(4) Martin, R. *Electronic Structure: Basic Theory and Practical Methods*; Cambridge Univerisity Press: Cambridge, U. K., 2004; pp 1−624.
(5) Koch, W.; Holthausen, M. C. *A Chemist's Guide to Density Functional Theory*; Wiley-VCH: New York, 2001; pp 1− 294.
(6) Hohenberg, P.; Kohn, W. *Phys. Rev.* **1964**, *136*, B864.
(7) Wang, Y.; Carter, E. A. In *Progress in Theoretical Chemistry and Physics*; Schwartz, S., Ed.; Kluwer: Dordrecht, The Netherlands, 2000; p 117.
(8) Perdew, J. P.; Burke, K.; Ernzerhof, M. *Phys. Rev. Lett.* **1996**, *77*, 3865.
(9) Perdew, J. P.; Ruzsinszky, A.; Csonka, G. I.; Vydrov, O. A.; Scuseria, G. E.; Constantin, L. A.; Zhou, X.; Burke, K. *Phys. Rev. Lett.* **2008**, *100*, 136406.
(10) Armiento, R.; Mattsson, A. E. *Phys. Rev. B* **2005**, *72*, 085108.
(11) Fabiano, E.; Constantin, L. A.; Della Sala, F. *Phys. Rev. B* **2010**, *82*, 113104.
(12) Fabiano, E.; Constantin, L. A.; Della Sala, F. *J. Chem. Phys.* **2011**, *134*, 194112.
(13) Pearson, M.; Smargiassi, E.; Madden, P. A. *J. Phys. Condens. Matter* **1993**, *5*, 3221.
(14) Smargiassi, E.; Madden, P. A. *Phys. Rev. B* **1994**, *49*, 5220.
(15) Govind, N.; Wang, J.; Guo, H. *Phys. Rev. B* **1994**, *50*, 11175.
(16) Foley, M.; Madden, P. A. *Phys. Rev. B* **1996**, *53*, 10589.
(17) Wang, Y. A.; Govind, N.; Carter, E. A. *Phys. Rev. B* **1998**, *58*, 13465.
(18) Wang, Y. A.; Govind, N.; Carter, E. A. *Phys. Rev. B* **2001**, *64*, 129901.
(19) Watson, S. C.; Carter, E. A. *Comput. Phys. Commun.* **2000**, *128*, 67.
(20) Zhou, B.; Ligneres, V. L.; Carter, E. A. *J. Chem. Phys.* **2005**, *122*, 044103.
(21) Senatore, G.; Subbaswamy, K. R. *Phys. Rev. B* **1986**, *34*, 5754.
(22) Johnson, M. D.; Subbaswamy, K. R.; Senatore, G. *Phys. Rev. B* **1987**, *36*, 9202.
(23) Cortona, P. *Phys. Rev. B* **1991**, *44*, 8454.
(24) Cortona, P. *Phys. Rev. B* **1992**, *46*, 2008.
(25) Wesolowski, T. A.; Warshel, A. *J. Phys. Chem.* **1993**, *97*, 8050.
(26) Wesolowski, T. A. In *Chemistry: Reviews of Current Trends*; Leszczynski, J., Ed.; World Scientific: Singapore, 2006; Vol. 10; pp 1−82.
(27) Wesolowski, T. A.; Chermette, H.; Weber, J. *J. Chem. Phys.* **1996**, *105*, 9182.

(28) Huang, P.; Carter, E. A. *J. Chem. Phys.* **2006**, *125*, 084102.
(29) Hodak, M.; Lu, W.; Bernholc, J. *J. Chem. Phys.* **2008**, *128*, 014101.
(30) Elliot, P.; Cohen, M. H.; Wasserman, A.; Burke, K. *J. Chem. Theory Comput.* **2009**, *5*, 827.
(31) Neugebauer, J. *Phys. Rep.* **2010**, *489*, 1.
(32) Laricchia, S.; Fabiano, E.; Della Sala, F. *J. Chem. Phys.* **2010**, *133*, 164111.
(33) Goodpaster, J. D.; Ananth, N.; Manby, F. R.; Miller, T. F., III. *J. Chem. Phys.* **2010**, *133*, 084103.
(34) Wesolowski, T. A. *J. Chem. Phys.* **1997**, *106*, 8516.
(35) Wesolowski, T. A.; Tran, F. *J. Chem. Phys.* **2003**, *118*, 2072.
(36) Kevorkyants, R.; Dulak, M.; Wesolowski, T. A. *J. Chem. Phys.* **2006**, *124*, 024104.
(37) Dulak, M.; Wesolowski, T. A. *J. Mol. Model* **2007**, *13*, 631.
(38) Götz, A. W.; Beyhan, S. M.; Visscher, L. *J. Chem. Theory Comput.* **2009**, *5*, 3161.
(39) Beyhan, S. M.; Götz, A. W.; Jacob, C. R.; Visscher, L. *J. Chem. Phys.* **2010**, *132*, 044114.
(40) Fradelos, G.; Wesolowski, T. A. *J. Chem. Theory Comput.* **2011**, *7*, 213.
(41) Thomas, L. H. *Proc. Cambridge Phil. Soc.* **1926**, *23*, 542.
(42) Fermi, E. *Rend. Accad. Naz. Lincei* **1927**, *6*, 602.
(43) von Weizsäcker, C. F. *Z. Phys. A* **1935**, *96*, 431.
(44) Acharya, P. K.; Bartolotti, L. J.; Sears, S. B.; Parr, R. G. *Proc. Natl. Acad. Sci.* **1980**, *77*, 6978.
(45) DePristo, A. E.; Kress, J. D. *Phys. Rev. A* **1987**, *35*, 438.
(46) Ou-Yang, H.; Levy, M. *Int. J. Quantum Chem.* **1991**, *40*, 379.
(47) Thakkar, A. J. *Phys. Rev. A* **1992**, *46*, 6920.
(48) Vitos, L.; Skriver, H. L.; Kollár, J. *Phys. Rev. B* **1998**, *57*, 12611.
(49) Karasiev, V. V.; Ludeña, E. V.; Artemyev, A. N. *Phys. Rev. A* **2000**, *62*, 062510.
(50) Karasiev, V. V.; Trickey, S. B.; Harris, F. E. *J. Comput.-Aided Mater. Des.* **2006**, *13*, 111.
(51) Perdew, J. P.; Constantin, L. A. *Phys. Rev. B* **2007**, *75*, 155109.
(52) Constantin, L. A.; Ruzsinszky, A. *Phys. Rev. B* **2009**, *79*, 115117.
(53) Karasiev, V. V.; Jones, R. S.; Trickey, S. B.; Harris, F. E. *Phys. Rev. B* **2009**, *80*, 245120.
(54) Wang, L.-W.; Teter, M. P. *Phys. Rev. B* **1992**, *45*, 13196.
(55) Chai, J.-D.; Weeks, J. D. *Phys. Rev. B* **2007**, *75*, 205122.
(56) Garca-Aldea, D.; Alvarellos, J. E. *J. Chem. Phys.* **2008**, *129*, 074103.
(57) Garca-Aldea, D.; Alvarellos, J. E. *Phys. Rev. A* **2008**, *77*, 022502.
(58) Huang, C.; Carter, E. A. *Phys. Rev. B* **2010**, *81*, 045206.
(59) Garca-Aldea, D.; Alvarellos, J. E. *J. Chem. Phys.* **2007**, *127*, 144109.
(60) March, N.; Santamaria, R. *Int. J. Quantum Chem.* **1990**, *39*, 585.
(61) Lee, H.; Lee, C.; Parr, R. G. *Phys. Rev. A* **1991**, *44*, 768.
(62) March, N. *Electron Density Theory of Atoms and Molecules*; Academic Press: London, 1992; p 1.
(63) Oliver, G. L.; Perdew, J. P. *Phys. Rev. A* **1979**, *20*, 397.
(64) Lembarki, A.; Chermette, H. *Phys. Rev. A* **1994**, *50*, 5328.
(65) Perdew, J. P.; Wang, Y. *Phys. Rev. B* **1992**, *45*, 13244.
(66) Kirzhnitz, D. *Sov. Phys. JETP* **1957**, *5*, 64.
(67) Bernard, Y. A.; Dulak, M.; Kamiński, W.; Wesolowski, T. A. *J. Phys. A: Math. Theor.* **2008**, *41*, 055302.
(68) Tran, F.; Wesoloski, T. A. *Int. J. Quantum Chem.* **2002**, *89*, 441.
(69) Lacks, D. J.; Gordon, R. G. *J. Chem. Phys.* **1994**, *100*, 4446.
(70) Constantin, L. A.; Fabiano, E.; Laricchia, S.; Della Sala, F. *Phys. Rev. Lett.* **2011**, *106*, 186406.
(71) Elliott, P.; Lee, D.; Cangi, A.; Burke, K. *Phys. Rev. Lett.* **2008**, *100*, 256406.
(72) Zhang, Y.; Yang, W. *Phys. Rev. Lett.* **1998**, *80*, 890.
(73) Scott, J. *Philos. Mag.* **1952**, *43*, 859.
(74) Schwinger, J. *Phys. Rev. A* **1980**, *22*, 1827.
(75) Englert, B.-G.; Schwinger, J. *Phys. Rev. A* **1984**, *29*, 2339.
(76) Lee, D.; Constantin, L. A.; Perdew, J. P.; Burke, K. *J. Chem. Phys.* **2009**, *130*, 034107.
(77) Perdew, J. P.; Constantin, L. A.; Sagvolden, E.; Burke, K. *Phys. Rev. Lett.* **2006**, *97*, 223002.
(78) Hui, O.-Y.; Levy, M. *Phys. Rev. A* **1990**, *42*, 155.
(79) Levy, M.; Hui, O.-Y. *Phys. Rev. A* **1988**, *38*, 625–629.
(80) Wang, B.; Stott, M. J.; von Barth, U. *Phys. Rev. A* **2001**, *63*, 052501.
(81) Iikura, H.; Tsuneda, T.; Yanai, T.; Hirao, K. *J. Chem. Phys.* **2001**, *115*, 3540.
(82) Lastra, J. M. G.; Kaminski, J. W.; Wesolowski, T. A. *J. Chem. Phys.* **2008**, *129*, 074107.
(83) Jones, W.; Young, W. *J. Phys. C* **1971**, *4*, 1322.
(84) Vela, A.; Medel, V.; Trickey, S. B. *J. Chem. Phys.* **2009**, *130*, 244103.
(85) Clementi, E.; Roetti, C. *Atomic Data Nucl. Data Tables* **1974**, *14*, 177.
(86) Constantin, L. A.; Snyder, J. C.; Perdew, J. P.; Burke, K. *J. Chem. Phys.* **2010**, *133*, 241103.
(87) Wesolowski, T. A.; Warshel, A. *Chem. Phys. Lett.* **1996**, *258*, 71.
(88) *TURBOMOLE*, V6.2; University of Karlsruhe and Forschungszentrum Karlsruhe GmbH: Karlsruhe, Germany, 1989−2007; TURBOMOLE GmbH: Karlsruhe, Germany, 2009.
(89) Rappoport, D.; Furche, F. *J. Chem. Phys.* **2010**, *133*, 134105.
(90) Weigned, F.; Ahlrichs, R. *Phys. Chem. Chem. Phys.* **2005**, *7*, 3297.
(91) Zhao, Y.; Truhlar, D. G. *J. Phys. Chem. A* **2005**, *109*, 5656.
(92) Zhao, Y.; Truhlar, D. G. *J. Chem. Theory Comput* **2005**, *1*, 415.
(93) Zupan, A.; Burke, K.; Ernzerhof, M.; Perdew, J. P. *J. Chem. Phys.* **1997**, *106*, 10184.
(94) Treutler, O.; Ahlrichs, R. *J. Chem. Phys.* **1995**, *102*, 346.
(95) Iyengar, S. S.; Ernzerhof, M.; Maximoff, S. N.; Scuseria, G. E. *Phys. Rev. A* **2001**, *63*, 052508.
(96) Murphy, D. R. *Phys. Rev. A* **1981**, *24*, 1682.
(97) Tran, F.; Wesolowski, T. A. *Chem. Phys. Lett.* **2002**, *360*, 209.
(98) Jacob, C. R.; Beyhan, S. M.; Visscher, L. *J. Chem. Phys.* **2007**, *126*, 234116.
(99) Boys, S. F.; Bernardi, F. *Mol. Phys.* **1970**, *19*, 553.
(100) Jacob, C. R.; Visscher, L. *J. Chem. Phys.* **2008**, *128*, 155102.
(101) Kiewisch, K.; Eickerling, G.; Reiher, M.; Neugebauer, J. *J. Chem. Phys.* **2008**, *128*, 044114.
(102) Govind, N.; Sushko, P.; Hess, W.; Valiev, M.; Kowalski, K. *Chem. Phys. Lett.* **2009**, *470*, 353.
(103) Fux, S.; Jacob, C. R.; Neugebauer, J.; Visscher, L.; Reiher, M. *J. Chem. Phys.* **2010**, *132*, 164101.
(104) Zhao, Q.; Morrison, R. C.; Parr, R. G. *Phys. Rev. A* **1995**, *50*, 238.
(105) Wu, Q.; Yang, W. *J. Chem. Phys.* **2003**, *118*, 2498.
(106) Roncero, O.; de Lara-Castells, M. P.; Villarreal, P.; Flores, F.; Ortega, J.; Paniagua, M.; Aguado, A. *J. Chem. Phys.* **2008**, *129*, 184104.
(107) Roncero, O.; Zanchet, A.; Villarreal, P.; Aguado, A. *J. Chem. Phys.* **2009**, *131*, 234110.
(108) Goodpaster, J. D.; Barnes, T. A.; Miller, T. F., III. *J. Chem. Phys.* **2011**, *134*, 164108.
(109) Chan, G. K.-L.; Handy, N. C. *J. Chem. Phys.* **2000**, *112*, 5639.